


RESEARCH ARTICLE

WILEY

FDEM and ERT measurements for archaeological prospections at Nuraghe S'Urachi (West-Central Sardinia)

Rita Deiana¹  | Gian Piero Deidda² | Enrique Díes Cusi³ | Peter van Dommelen⁴ | Alfonso Stiglitz⁵

¹Department of Cultural Heritage, University of Padova, Padova, Italy

²Department of Civil and Environmental Engineering and Architecture, University of Cagliari, Cagliari, Italy

³Independent Scholar, Valencia, Spain

⁴Joukowsky Institute for Archaeology and the Ancient World, Brown University, Providence, Rhode Island, USA

⁵Comune di San Vero Milis, Museo Civico, San Vero Milis, Italy

Correspondence

Rita Deiana, Department of Cultural Heritage, University of Padova, Piazza Capitaniato 7, Padova, Italy.
Email: rita.deiana@unipd.it

Funding information

Loeb Classical Library Foundation (Harvard University); Comune and Museo Civico di San Vero Milis; Brown University, Joukowsky Institute for Archaeology and the Ancient World

Abstract

Nuraghe S'Urachi is a monumental architectural complex in West Central Sardinia that was probably first built in the Bronze Age and remained occupied continuously into the early Roman Imperial period. It has been the object of systematic and large-scale archaeological investigations in three different phases since 1948 when the first excavations revealed a complex building within a massive defensive wall and multiple towers. Intermittent fieldwork between the 1980s and 2005 subsequently showed that the central nuraghe might comprise up to five principal towers. In 2013, a new collaborative research project, sponsored by Brown University and the Municipality of San Vero Milis, brought together a multidisciplinary research project to investigate this important archaeological site. In this framework, multi-frequency and multi-coil electromagnetic measurements (FDEM) and Electrical resistivity tomography (ERT) were carried out in 2018, 2019, and 2020, over and close to the nuraghe towers, to gain a better understanding of the inner part of the main structure and to investigate the surrounding area that was intensively settled in Phoenician and Punic times. The preliminary results of the geophysical measurements provide new and interesting evidence that supports new hypotheses and suggests possible future archaeological and geophysical strategies to investigate the unexcavated part of the archaeological site of S'Urachi.

KEYWORDS

electrical resistivity tomography, multi-coil electromagnetic measurements, multi-frequency electromagnetic measurements, Nuraghe, Phoenician, Sardinia

1 | INTRODUCTION

Geophysical measurements have supported archaeological research for decades, allowing the collection, in a non-invasive way, of information on any possible buried structure in a specific site (Batayneh, 2011; Clark, 2000; R. Deiana, 2019; R. Deiana, Bonetto, et al., 2018; El-Qady et al., 2019; Kvamme, 2003; Schmidt, 2001; Wynn, 1986). Regardless of subsequent excavation and generally starting from

historical information or data provided by previous archaeological surveys, identifying selected targets or the extent of entire buried settlements is the main objective of geophysical prospecting. This paper similarly presents the preliminary results of the combined use of electrical resistivity tomography (ERT) and frequency domain electromagnetic measurements (FDEM) as applied at Nuraghe S'Urachi, in central west Sardinia (Figure 1). Nuraghi are 'Cyclopean' indigenous dry stone-built settlement towers constructed in large

This is an open access article under the terms of the Creative Commons Attribution License, which permits use, distribution and reproduction in any medium, provided the original work is properly cited.

© 2021 The Authors. *Archaeological Prospection* published by John Wiley & Sons Ltd.

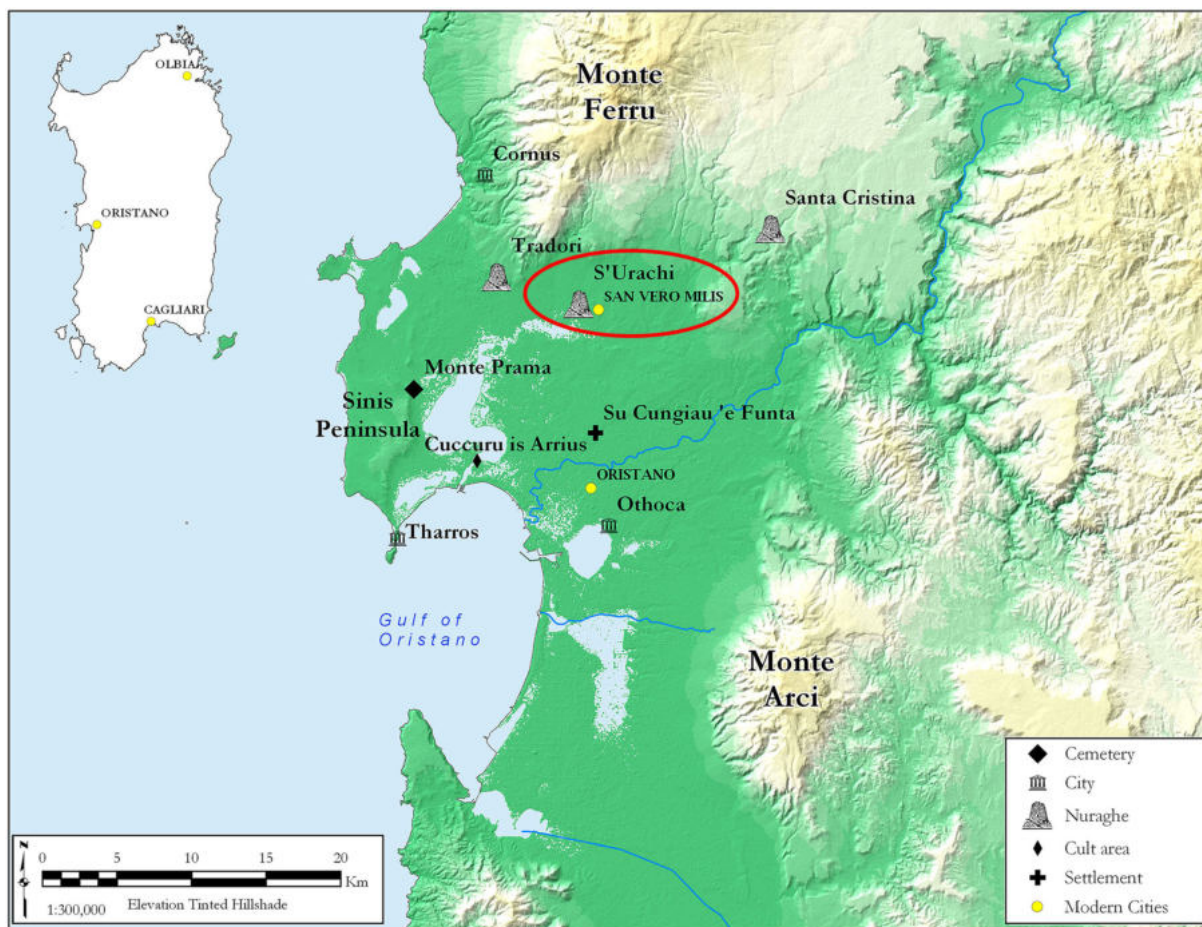


FIGURE 1 Map of west central Sardinia, showing the location of S'Urachi and other significant sites (drawing Jessica Nowlin) [Colour figure can be viewed at wileyonlinelibrary.com]

numbers across Sardinia from the Bronze Age. There are well over 7,000 nuraghi on record across the island, invariably considered prehistoric monuments first built in the Bronze Age. They continued to be inhabited for much longer, however, well into historical times.

Nevertheless, even if the ‘monuments’ afterlives have often been acknowledged, they have rarely been investigated in their own right. Although most nuraghi are modest single towers, a small number are complex multi-towered monuments, and S'Urachi is among the largest of these (Lilliu, 1988; Minoja et al., 2015; Webster, 2015). Excavations in 1948, directed by Giovanni Lilliu, and in the 1980s under Giovanni Tore's supervision, have revealed an elaborate monument with up to five towers and surrounded by an outer circuit wall that includes 10 towers (A. Stiglitz et al., 2015; Figure 2). These earlier excavation campaigns have made it clear that the site was occupied for most of the time between the Middle Bronze Age and the early Roman Imperial period—including the Phoenician and Carthaginian colonial occupation between the 8th and 3rd centuries BCE (Stiglitz, 2019). Renewed fieldwork of the ‘Progetto S'Urachi’ (sponsored by the Museo Civico of San Vero Milis (Sardinia, Italy) and the Joukowsky Institute of Archaeology and the Ancient World (Rhode Island, USA)), has demonstrated not only that the area around the nuraghe was

continuously inhabited throughout the first millennium BCE but also that the monument itself was substantially modified by the construction of new open spaces and rooms (P. van Dommelen et al., 2020).

In this framework, three ERT and FDEM fieldwork campaigns (Figures 3 and 4) were undertaken between 2018 and 2020 with the double objective to investigate the inner part of the un-excavated nuraghe and to gain an overview of buried archaeological features in its immediate surroundings.

The electrical resistivity method, widely used in archeology, generally allows the identification of buried structures in both conductive and resistive systems (M.A. Berge, Drahor, 2011a, 2011b; Mol & Preston, 2010; P.I. Tsourlos & Tsokas, 2011; Walker, 2000; Ullrich et al., 2007). The scientific literature concerning the applications of ERT measurements in archaeology shows increasing use of this technique in the last 20 years, in 2D and 3D configurations. ERT measurements are also often combined with other geophysical methods in different contexts to achieve excellent results (Bernardes et al., 2017; R. Deiana, Leucci, et al., 2018; Himi et al., 2016; Papadopoulos et al., 2006).

The FDEM method and the ERT method, in general, can provide information on the distribution of electrical conductivity (Bonsall et al., 2013; P. De Smedt et al., 2013, 2014; T. Saey et al., 2012,

FIGURE 2 Aerial (drone) view of nuraghe S'Urachi: excavation area D is to the left of the image; E is at the bottom centre; excavation area F is not shown on this photo. See Figure 6 for further details of tower labels and excavations areas (photo Fabrizio Pinna) [Colour figure can be viewed at wileyonlinelibrary.com]



2013; A. Tabbagh, 1986, 1990) or, its inverse, the electrical resistivity of the subsurface and any buried bodies in a given system (Dabas & Tabbagh, 2003; James et al., 2003; Rhoades et al., 1989). However, whereas FDEM measurements can provide mapping of conductivity or resistivity at several depths over large areas, the ERT method is dedicated to clarify the lateral and vertical distribution of this parameter in specific limited areas. In general, then, based on these considerations, ERT measurements are not infrequently used later to detail what has been identified extensively and qualitatively by FDEM prospecting. However, this possibility of joint application lacks whenever one has to investigate a very resistive system ($>500 \Omega\text{m}$). This limitation excludes the possibility of applying ERT and FDEM techniques simultaneously in highly resistive soils (Thiesson et al., 2009), where ERT measurements only suffer from the restriction of a possibly difficult electrical contact between the electrodes and the terrain. Then, where it is possible, the integration of FDEM and ERT methods appears successful, particularly in complex archaeological situations (Bonsall et al., 2013; P. De Smedt et al., 2013, 2014; T. Saey et al., 2012, 2013; A. Tabbagh, 1986, 1990) and where unfavourable logistics complicate the use of automated resistivity systems (e.g., ARP *Geocarta* SA, France). This holds true, in particular, when

considering both the speed of FDEM data acquisition and the degree of detail and in-depth control of the ERT method (R. Deiana et al., 2020; Vacilotto et al., 2020), which are fundamental attributes that especially relevant at complex archaeological sites such as S'Urachi, where logistics and archaeological issues can benefit from this combination. The use of other survey methods generally applied in archaeological contexts, such as the GPR method and the magnetic method were not considered on this occasion within the scope of this study in light of the results of some tests conducted with the same methods in the area during the 2014 excavation campaigns by Eastern Atlas GmbH & Co (Gosner & Smith, 2018). In fact, the GPR and magnetic gradient data acquired here were found to be poorly informative due to the particularly unfavourable signal-to-noise ratio related to the characteristics of the area. In particular, in fact, as far as the magnetic method is concerned, the presence of a high amount of scattered material of volcanic origin and the presence of a considerable amount of metallic waste still present in the area do not allow to obtain a good result with this technique in the area. On the other hand, the same presence of collapsed material and a large amount of garbage in the area overshadow the signal of residual archaeological structures expected at the foot of the nuraghe, such as those



FIGURE 3 Position of the five ERT lines collected at S'Urachi during geophysical fieldwork in 2018 and 2019. Note that excavation area F had not yet been opened when the aerial photo was taken; it is crossed by line L2 [Colour figure can be viewed at wileyonlinelibrary.com]

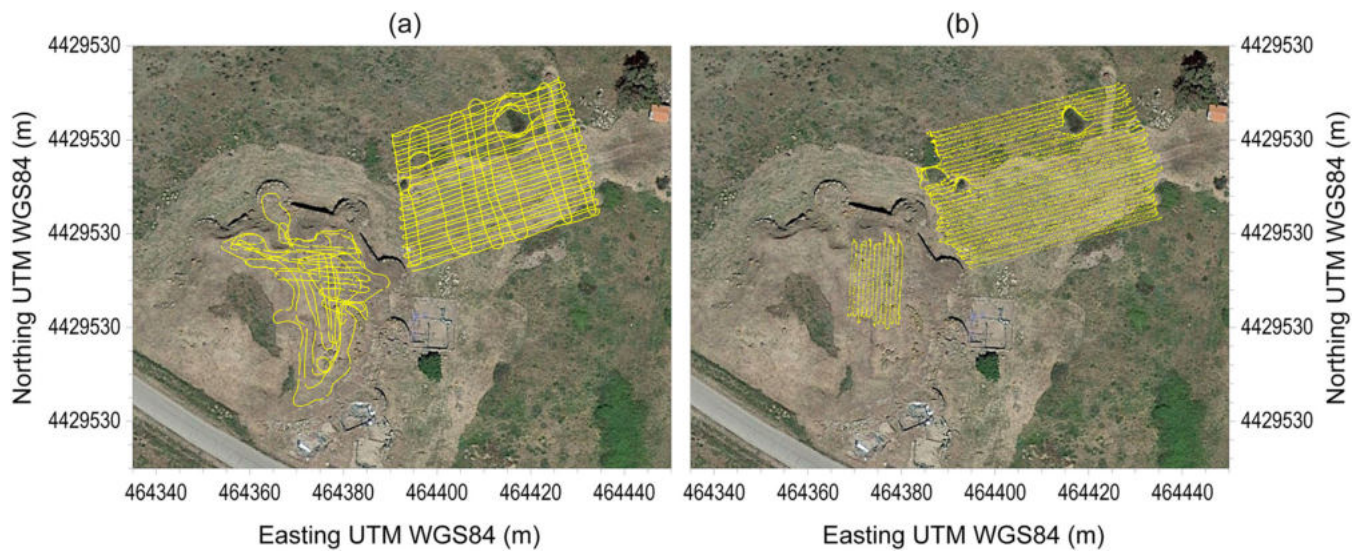


FIGURE 4 Position of the FDEM measurement paths in 2018 (a) with the GEM-2 and in 2019 (b) with the CMD Mini-explorer, inside and outside the Nuraghe. Note that excavation area F had not yet been opened when the aerial photo was taken; it would be located at the centre top of the photo [Colour figure can be viewed at wileyonlinelibrary.com]

identified in the excavation of area F (Figure 6) which are difficult to detect under these conditions.

1.1 | Study area

The site of S'Urachi is located in the low-lying and the gently rolling plain of the Campidano di Milis, which runs roughly east–west between the towering massif of the Montiferru, an extinct volcano to the north, and the Cabras wetlands to the south—(early) modern land reclamations have radically altered the latter landscape since Antiquity, but even so, ponds, lagoons and salt marshes remain sufficiently frequent features to give an impression of its erstwhile character (Figure 1). The region is dissected by numerous water-rich streams running off the slopes of the Montiferru into the wetlands; it was also densely occupied by nuraghi (Vanzetti et al., 2013; Figure 5).

As a simplified soil map of the immediate environs of the site shows, S'Urachi sits at the transition from coarse stony soils in the east to deeper, well developed and more easily workable soils in the western reaches of the Campidano di Milis (Figure 5). The site is located on the edge of the southward-stretching lower terrace of the Montiferru basalts, whose shallow and stony soils are poorly suited for agricultural exploitation. However, it affords a good vantage point overlooking the low-lying stream valleys and wetlands, a frequently recurring choice of location for major nuraghi (A. Depalmas & Melis, 2010).

The site has seen three principal phases of excavation that have targeted different areas and aspects of the monument. In 1948, Giovanni Lilliu focused his efforts on the outer defensive wall (*antemurale*) that he brought to light for most of its perimeter, thus demonstrating the remarkable size and standardized layout of the monument in what are presumed to be its later stages by the end of the 2nd millennium BCE. Because the nuraghe itself is contained within the *antemurale*, which is assumed to represent a later addition, and had remained entirely invisible, new excavations were started on the top of the monument by Giovanni Tore, which continued for most of the 1980s. Multiple years of fieldwork yielded vast quantities of finds from many different periods, which showed that many centuries of mudbrick production and stone extraction in recent centuries had seriously compromised the upper part of the monument. In the final campaign of 1995, the contours of a large tower and an elongated wall emerged, suggesting that the nuraghe is unlikely to have stood at the centre of the space enveloped by the *antemurale* (Figure 6: tower A). Comparison to nuraghe Su Nuraxi of Barumini has been a reason to propose that S'Urachi may have been a four-towered complex. However, this interpretation was subsequently refuted by the results of the 2005 excavation season when Alfonso Stiglitz and Alessandro Usai found traces of another tower in a location that is incompatible with the four-tower plan (Figure 6: tower B). Although it is clear that the nuraghe of S'Urachi must be multi-towered and possibly may have counted as many as five towers, its plan remains uncertain (A. Depalmas, 2015; A. Stiglitz et al., 2012; Vanzetti et al., 2013; Figure 7).

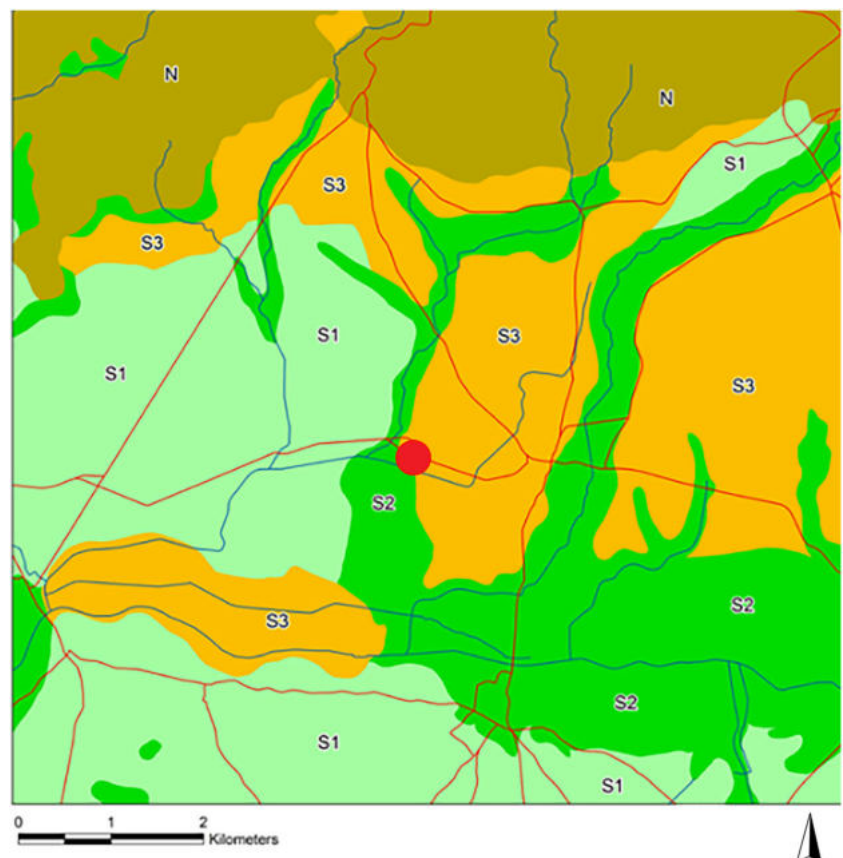


FIGURE 5 Simplified soil map of the immediate surroundings of S'Urachi, indicating the soil suitability for agriculture. Legend: S1, highly suitable; S2, moderately suitable; S3, marginally suitable; N, not suitable. The red dot at the centre of the map indicates the location of S'Urachi (map prepared by Antonia Arnoldus-Huyzenveld, Tiziano Abba, and Cristiano Nicosia for the S'Urachi Project in 2015) [Colour figure can be viewed at wileyonlinelibrary.com]

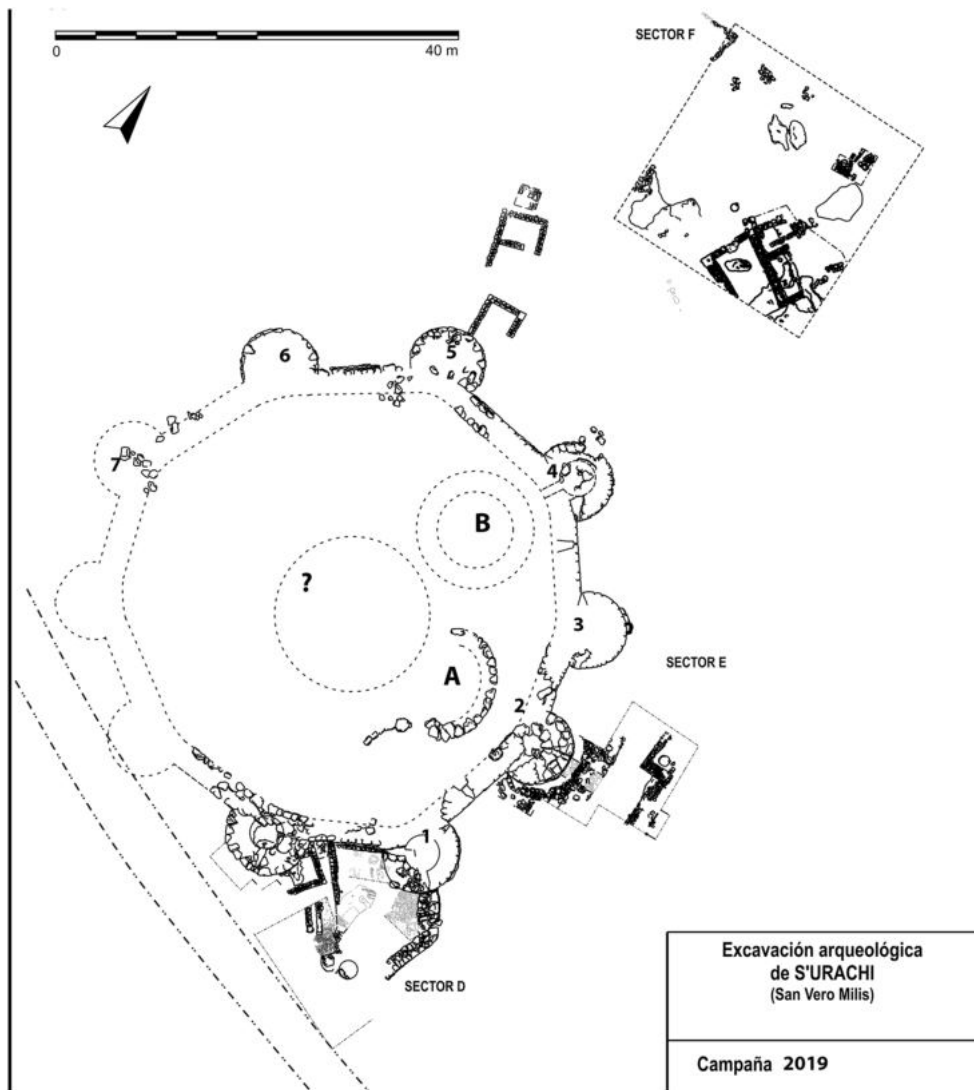


FIGURE 6 Overview plan of the Nuraghe complex and excavations areas at S'Urachi, showing the state of fieldwork in 2019 (drawing by Enrique Díes Cusi)



FIGURE 7 Reconstruction of S'Urachi in Punic times, showing the surrounding village in the foreground and the Nuraghe contained by the outer defensive wall in the background (view from the north, coinciding with excavation area F; see also Figure 6; reconstruction and drawing by Enrique Díes Cusi; colour illustration by Clara Díes Valls) [Colour figure can be viewed at wileyonlinelibrary.com]

The final and third phase of fieldwork started in 2013 with the *Progetto S'Urachi*. At this time, efforts have been targeted on the area immediately surrounding the nuraghe because the later stages of the occupation tend to be found in the so-called village around the monumental complex. Chance finds, systematic surveying, including geophysical prospection, and recent stratigraphic soundings show that an area reaching as far as 150 m away from the nuraghe may have been built up, and occupied between the later Bronze Age and the end of the Punic period, i.e. throughout the first millennium BCE (Gosner & Smith, 2018; Madrigali et al., 2019; Figure 7).

The *Progetto S'Urachi* has been excavating in three areas outside the monumental complex (A. Stiglitz et al., 2015; P. van Dommelen et al., 2018, 2020). Both areas D and E (Figure 6) are located immediately adjacent to the outer defensive wall, the former to the south and the latter to the east. Area F is instead located at around 50 m distance from the outer wall to the north (Figure 6).

Area D is defined by a complex accumulation of some major and numerous minor walls that have repeatedly modified the spatial organization and architectural make-up of this area, effectively adding a new wing to the monument around the 8th century BCE, more or less around the time that the Phoenicians arrived in Sardinia, including in the Gulf of Oristano. Area E is, on the contrary, a much more open area, as it is dominated by a large ostensibly defensive ditch that was

built in the late 8th century BCE. The ditch was gradually backfilled with domestic refuse from the early 7th century onwards and eventually partially built over by the 4th century. Area F is yet again quite different, as it appears to be a primarily domestic area, where excavations have begun to bring to light a multi-roomed house. Two test trenches indicate that the depth of archaeological deposits may be as deep as 2 m below the present surface.

As already discussed, the nuraghe contained within the outer defensive wall is almost entirely unknown. Given the size of the area within the outer wall (~1,300 m²), it is assumed that the nuraghe may comprise a plurality of towers, two of which are currently visible. Heavy quarrying over the past centuries to build houses in nearby San Vero Milis has revealed that the SW portion is devoid of any structures, suggesting that it could be the area of a large courtyard.

The ditch discovered in area E is a unique feature in Nuragic archaeology. Geophysical prospection around nuraghe Sant'Imbenia (Alghero, northeast Sardinia) has detected a 'channel' at some distance from the nuraghe, but there is no indication of a stone embankment (Johnson, 2012). Evidence of comparable stone-lined ditches can be found outside Sardinia, in particular in the Phoenician world, such as at the site of La Pícola (Santa Pola) on the Mediterranean coast of southeast Iberia (Lorrio, 2012).

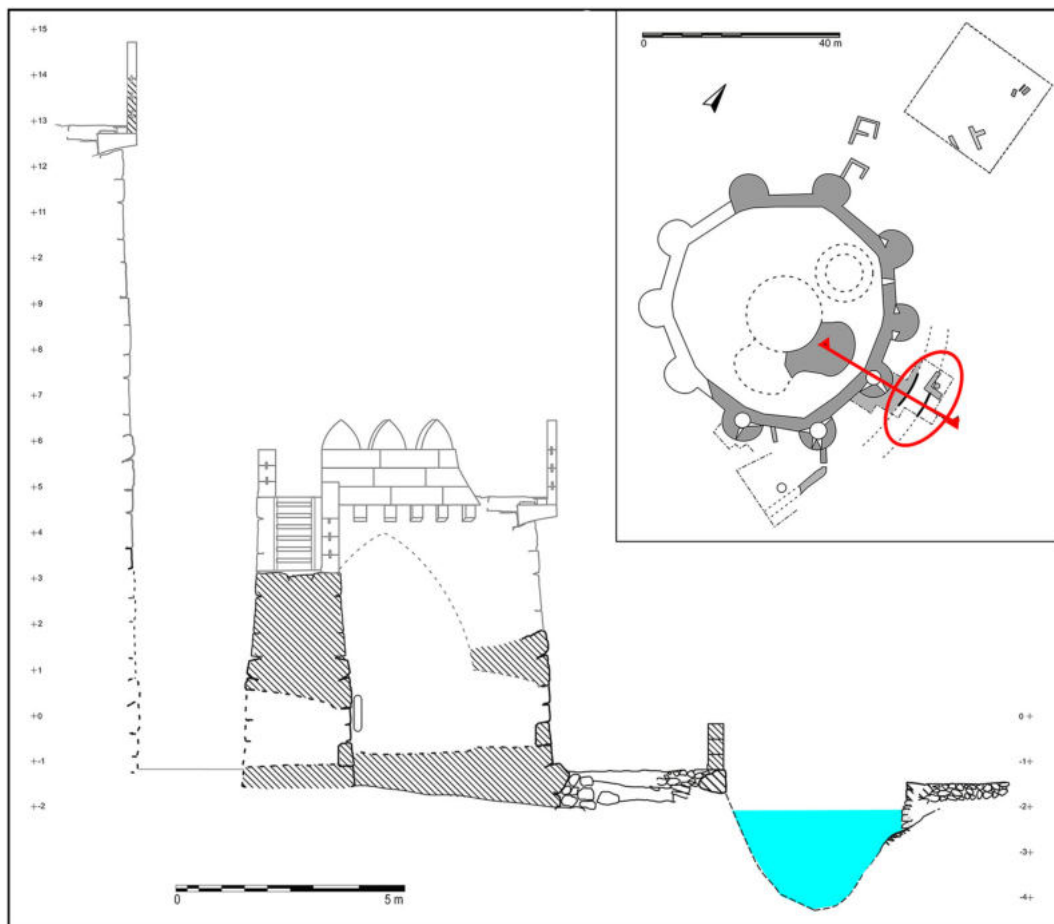


FIGURE 8 Section of area E, showing the ditch and associated tower (#2) of the outer defensive wall of S'Urachi; the insert shows the location of area E in relation to the Nuraghe as a whole (drawings by Enrique Dies Cusi) [Colour figure can be viewed at wileyonlinelibrary.com]

The excavations at S'Urachi show that the stone embankments were built in association with the outer defensive wall, and it is, therefore, reasonable to assume that the ditch was part of that defensive project (Figures 8 and 9). The high local water table suggests that it is also possible that the ditch was constructed to channel an existing stream and presumably manage the risks of flooding and erosion. The excavations have exposed the western

embankment for a maximum length of 12 m, and the slight curve suggests that the ditch might follow the outer defensive wall and thus possibly surround the entire complex (Figures 8 and 9).

2 | GEOPHYSICAL MEASUREMENTS

Because the extent of the areas under excavation is inevitably limited by the intensive nature of the archaeological investigation, geophysical prospection offers the means to examine (literally) in some depth a much broader portion of the site. There are three critical questions that the excavation cannot (yet) fully address, namely, the nuraghe itself, the ditch in area E and the houses in area F. An initial campaign of geophysical prospection in 2014 using magnetometry recorded a dense and extensive patchwork of anomalies but was unable to document many details (Madrigali et al., 2019; A. Stiglitz et al., 2015).

The first aim of the geophysical prospection, carried out between 2018 and 2020 using ERT and FDEM resistivity measurements, has been to shed light on the make-up of the nuraghe contained within the outer wall and to ascertain the course followed by the ditch in area E as the second aim. Finally, the third objective dovetails with the excavations begun in area F where two deep stratigraphic soundings have indicated that substantial archaeological deposits can be found as deep as 2 m below the present-day surface. Current excavations are concentrated in the southeast corner of the area and have only touched the upper layers (Figure 10).

2.1 | Electrical resistivity tomography (ERT)

The first test with ERT measurements in the S'Urachi area was carried out in July 2018 with the acquisition of one ERT line (L1 in Figure 3) in SW-NE direction at the base of the nuraghe, in a flat area east of area F. This ERT profile was acquired using a Syscal Pro Switch 48 (Iris Instruments) resistivity metre, laying out 48 electrodes spaced

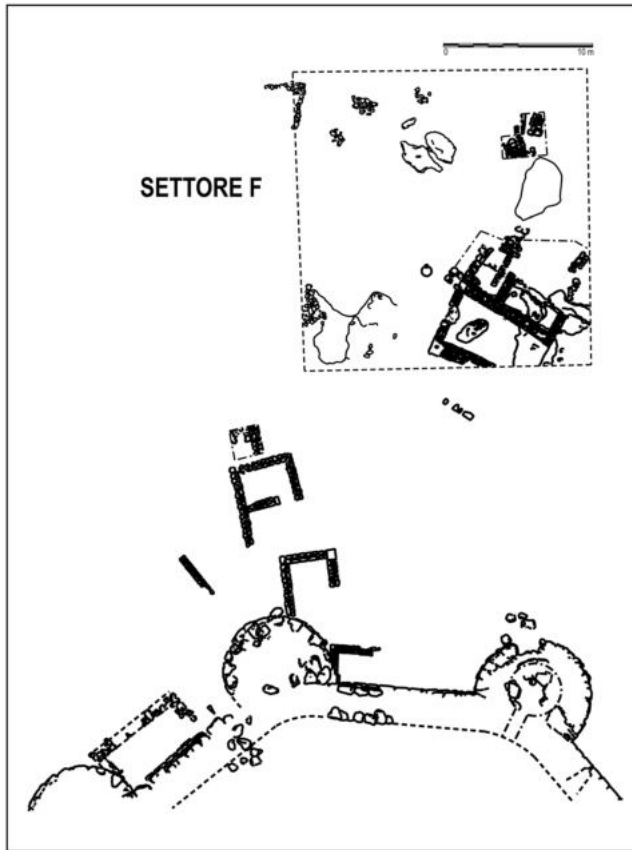


FIGURE 9 Plan of area F and nearby stretch of the outer defensive wall of S'Urachi (drawing by Enrique Díes Cusí)

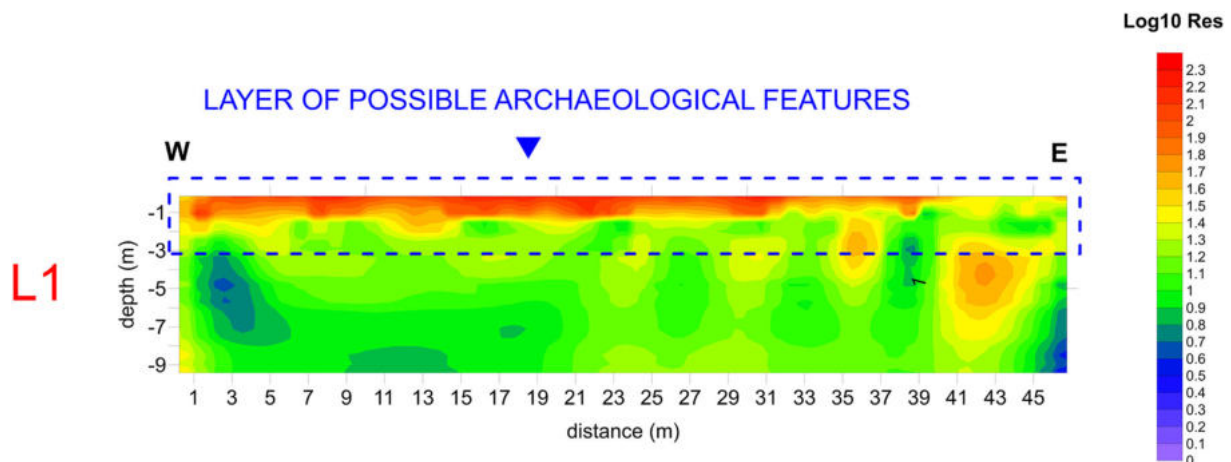


FIGURE 10 Result of ERT line L1 collected in 2018 outside the Nuraghe (see Figure 3 for the position) [Colour figure can be viewed at wileyonlinelibrary.com]

1 m apart and adopting a 'skip 4' dipole-dipole quadrupole array in order to optimize and balance the resolution capability and signal strength. The 'skip' in general refers to the number of electrodes skipped within a dipole, for both current and potential electrodes, so that 'skip 4' means four electrodes (or five minimum electrode distances) separating a couple of electrodes used for current injection from these one used for voltage measurements. Increasing the potential dipole spacing increases the magnitude of the measured voltage, enhancing the signal-to-noise ratio. A small electrode spacing, instead, means high-resolution capability. Besides, increasing the current dipole spacing increases the depth of investigation, which reached the value of about 9 m in the present case. Taking advantage of the stacking capability of the Syscal Pro resistivity metre, for each quadrupole, the measurements were repeated from a minimum of three to a maximum of six times to get data with a standard deviation (stacking error or quality factor) of no more than 5%. The duration of each measurement cycle was 250 ms, whereas the current injection was automatically corrected to obtain a reading of the voltage of at least 50 mV. In addition, direct and reciprocal measurements were made by interchanging the potential electrodes with the current electrodes to estimate better the measurement errors (Daily et al., 2004), checking the validity of the reciprocity theorem (Parasnis, 1988). The dataset for this profile was composed of 2,207 measurements (including direct and reciprocal measurements).

Four ERT lines (L2–L5) were acquired across the nuraghe (Figure 3) in July 2019, using the same procedure and acquisition parameters as for line L1, except for the minimum electrode spacing, that for these lines was 2 m, with a total length of 94 m and an investigation depth of about 24 m. Given the difference in elevation of about 5 m between the top of the nuraghe and the terrain at the base of the surrounding defensive wall, the acquisition of the lines was complemented with measurements of the topographic positions of each electrode for each ERT line (P.I. Tsourlos et al., 1999), georeferenced by a Stonex S8 Plus Global Navigation Satellite System (GNSS).

ERT data inversions were performed using an Occam inversion approach (LaBrecque et al., 1996) using the ProfileR software package (Binley, 2008). Preliminary data processing consisted of rejecting data if the difference between direct and reciprocal measurements exceeded the quality factor for data recording. In general, this criterion implied a loss of approximately 10% of data points, ensuring maximum control over the validity of the data used in the inversion process.

2.2 | Frequency domain electromagnetic measurements (FDEM)

The FDEM survey was carried out between July 2019 and January 2020 due to some technical problems. The extension of the area around the nuraghe, the presence of a metallic fence in the western part and the high and dense vegetation forced the data collection in two separate areas. The first investigated area corresponding to a part of the top of the nuraghe, where the second one is at the foot of the nuraghe, in the north-east sector close to the excavation area F

(Figure 6). In this second area, investigated with FDEM measurements, in 2018, the first ERT line was collected (Figure 3a). In both areas, the FDEM survey was performed by using two different electromagnetic induction (EMI) devices: multi-frequency and multi-coil.

The first dataset was acquired using a multi-frequency Geophex GEM-2. In this instrument, the distance between the transmitter coil and the main receiver coil is 1.66 m, and multiple frequencies (up to 10, although it is advisable to select no more than five or six frequencies) ranging from 330 Hz to 93 kHz are used (F.-X. Simon et al., 2014). At S'Urachi, both quadrature and in-phase responses were recorded carrying the instrument in the horizontal coplanar (HCP) orientation at positioning it at 0.9 m above the ground surface and using six frequencies: $f_1 = 1,025$ Hz, $f_2 = 4,025$ Hz, $f_3 = 9,825$ Hz, $f_4 = 16,725$ Hz, $f_5 = 28,725$ Hz and $f_6 = 47,025$ Hz. In the Low Induction Number condition, the interest of multi-frequency EMI measurement is twofold: (1) it allows the determination of the magnetic viscosity (F.-X. Simon et al., 2015) and, of the effective dielectric permittivity (Simon et al., 2018), (2) confirms the conductivity magnitude and variations (see Figures 13 and 14 below). At the foot of the nuraghe, the FDEM data were collected using the GEM-2 oriented perpendicular to the walking path, along parallel lines every metre, using a 0.5 m sampling interval (Figure 4a). On the top of the nuraghe instead, the data were collected following an irregular path to best cover the surface amidst the high vegetation (Figure 4a).

The multi-coil dataset was collected using a GF Instruments CMD Mini-explorer. This device operates using a 30 kHz fixed frequency and a one transmitter coil paired with three coplanar receiver coils placed at 0.32, 0.71 and 1.18 m from the transmitter, allowing three simultaneous measurements of the apparent electrical conductivity. The three different receivers provide three different depths of investigations (DOI) for each possible coils orientation: horizontal coplanar (HCP) position provide about 0.5, 1.0 and 1.8 m investigation depth, where vertical coplanar (VCP) position provide 0.25, 0.50 and 0.90 m depth of investigation. The data were collected in continuous mode, with a 0.5 s time step, with the probe 0.2 m above the ground, first orienting in horizontal, then in vertical position. The survey areas collected in two different periods (July 2019 for GEM-2 and January 2020 for the CMD-Mini explorer), with other vegetation conditions, are only partial coincident (Figure 4b).

All measurements have been properly georeferenced using a Stonex S8 Plus GNSS to obtain the right evaluation and correlation between any possible anomaly and the position and orientation of the visible and documented archaeological structures in the adjacent excavated area F.

3 | RESULTS AND DISCUSSION

3.1 | ERT

The results of the electrical resistivity tomography acquired at the base and on top of the nuraghe in 2018 and 2019 are presented

respectively in Figures 10 and 11. To allow adequate comparison between the anomalies present in the different sections, we adopted a common log₁₀ resistivity range for all sections (0–2.3 log₁₀ Res). The L1 section acquired in SW–NE direction below the nuraghe in 2018, to the east of excavation area F, enabled us to investigate the first 9 m below the present-day land surface.

In this section (L1 in Figure 10), there is a clear increase in resistivity in the first meter and a half of depth. Because this section coincides with a solidly compacted dirt road that is probably

rich in coarse materials to give stability to the substrate, it prevents the clear identification and separation of any possible smaller structural remains, just below this upper resistive layer. The question whether the structures of sector F extend to the east is instead confirmed by the anomalies identified in the NE portion of the ERT section L4.

The four ERT sections acquired in 2019 (Figures 3 and 11), however, are most interesting and highly significant, as they identify larger structures both inside and outside the nuraghe.

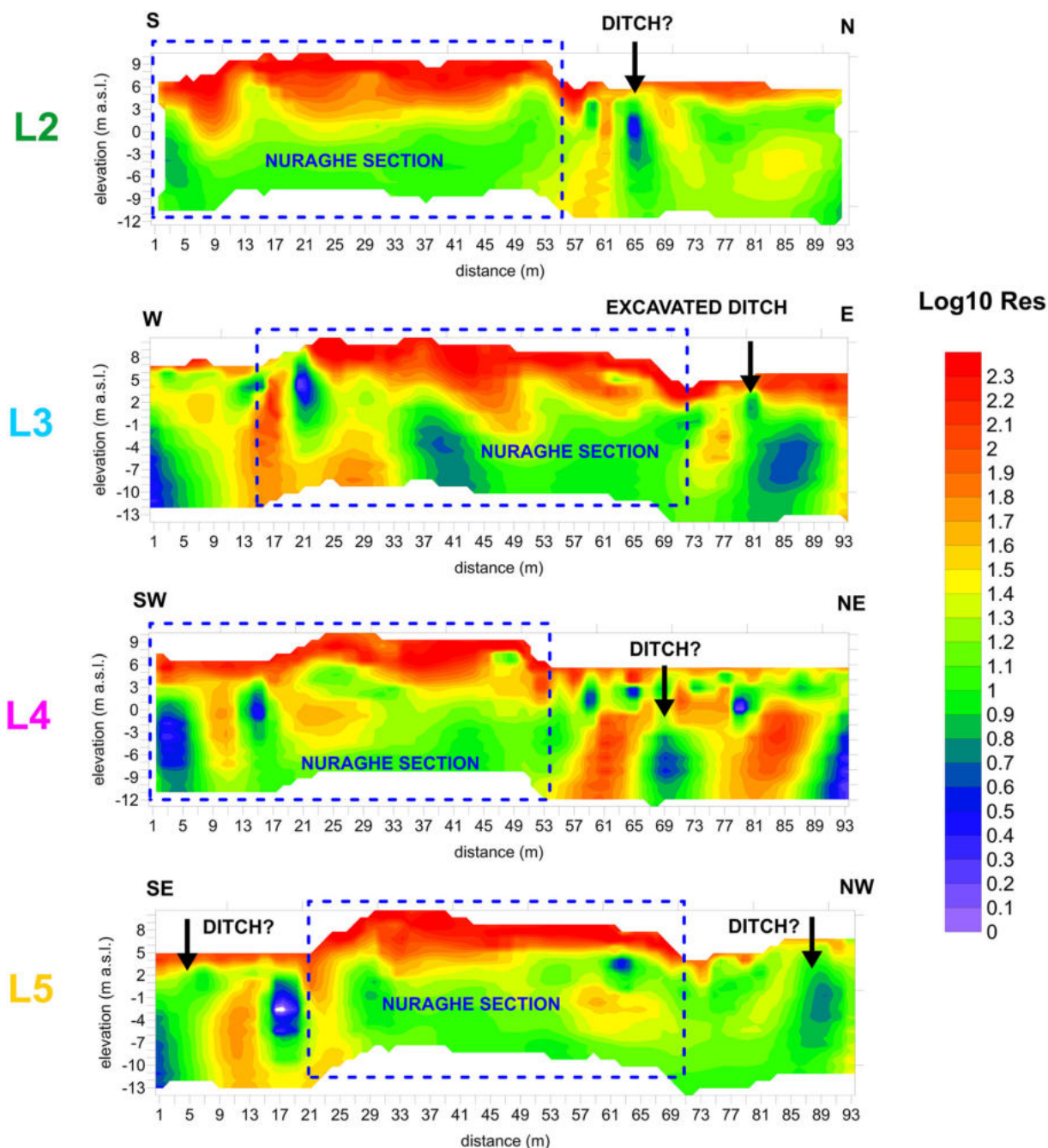


FIGURE 11 Results of ERT lines (L2–L5) collected in 2019 across the nuraghe (see Figure 3 for the position) [Colour figure can be viewed at wileyonlinelibrary.com]

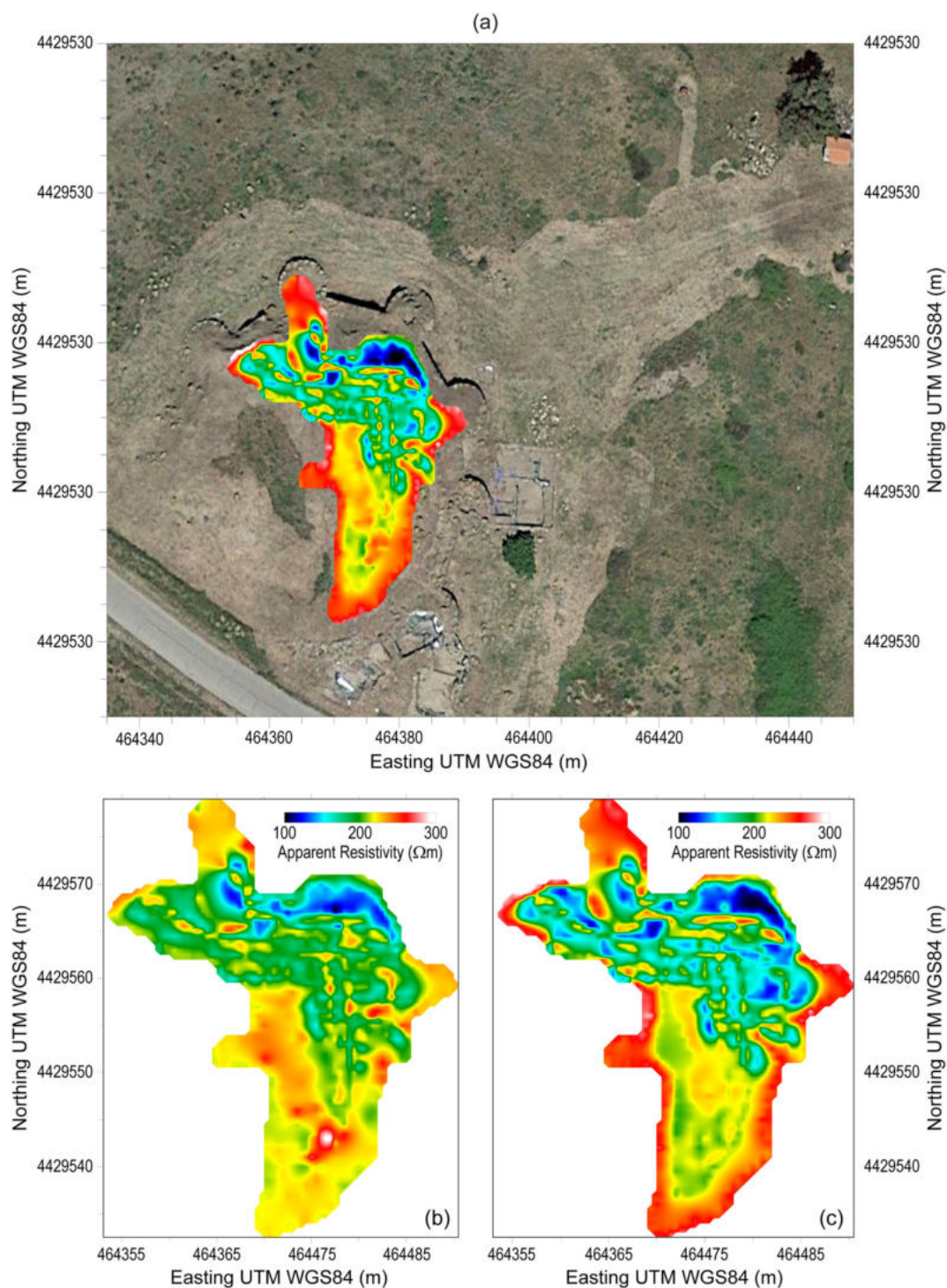


FIGURE 12 Maps of apparent resistivity by the quadrature component of the EM signal above the Nuraghe: (a) frequency 4,025 Hz, (b) frequency 9,825 Hz, and (c) frequency 47,025 Hz collected in 2019 with GEM 2 in HCP configuration. All images use the same resistivity range [Colour figure can be viewed at wileyonlinelibrary.com]

Line L2 intersects the nuraghe in south–north direction, continuing across excavation area F (Figures 3–6). The high variability of electrical resistivity within the nuraghe supports the presence of several broader features that may well represent towers partially filled with collapsed building materials, especially in the top part where the highest resistivity values are seen. The blue dotted box in the ERT

images in Figure 11 indicates the area occupied by the nuraghe in each section. The conductive anomaly just to the north of the nuraghe at approximately 65 m is also interesting because it possibly represents the continuation of the ditch excavated in area E.

The results from the four ERT sections across the nuraghe are consistent with suggesting that the complex contains several

structures (i.e., towers). These could be filled with soil or be hollow spaces. Section L3 moreover shows a remarkable anomaly practically centrally located within the nuraghe that probably represents a well because it sits at a depth that roughly matches the level of the groundwater table in the ditch of excavation area E.

Highly significant is that all other ERT sections (L2, L4 and L5 in Figure 11) show low resistivity anomalies at a short distance beyond the outer wall of the nuraghe, which is compatible with the position and resistivity values of the ditch excavated in area E. Together, the ERT sections thus strongly suggest that the ditch continued on either

side of excavation are E and surrounded the nuraghe almost entirely—the tarmac road to the south of the nuraghe makes ERT investigation of that sector impossible.

3.2 | FDEM

The results of the FDEM investigations carried out with the two instruments on top of the nuraghe and to the north-east of the monument are presented in Figures 12–15.

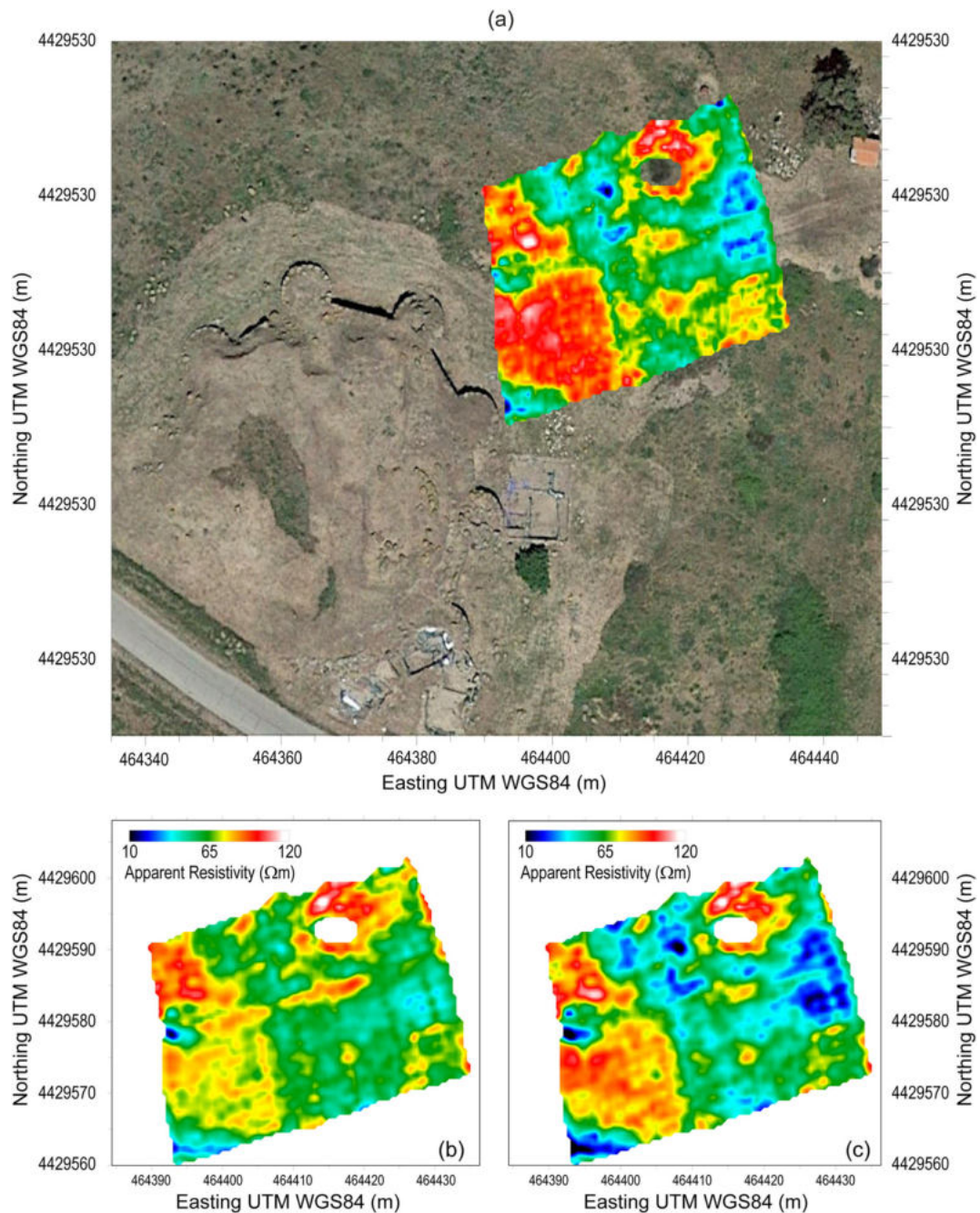


FIGURE 13 Maps of apparent resistivity by the quadrature component of the EM signal at the foot of the Nuraghe (a) frequency 16,725 Hz, (b) frequency 28,725 Hz, and (c) frequency 47,025 Hz collected in 2019 with GEM 2 in HCP configuration. All images use the same resistivity range [Colour figure can be viewed at wileyonlinelibrary.com]

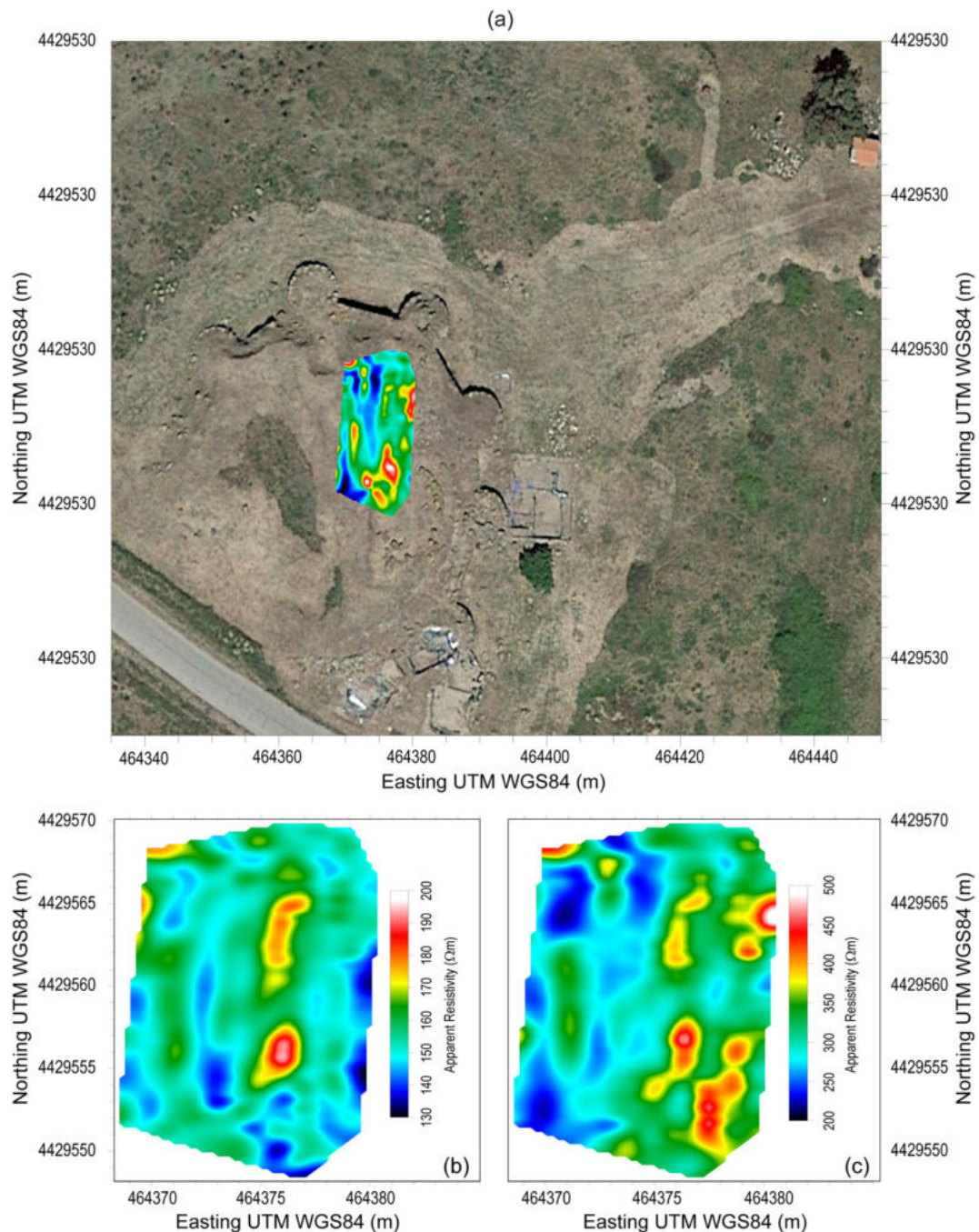


FIGURE 14 Maps of apparent resistivity above the Nuraghe collected in 2020 using the CMD Mini explorer in VCP configuration over different terrain thicknesses: (a) 0.9 m DOI (resistivity range 150–300 Ωm), (b) 0.25 m DOI (resistivity range 130–200 Ωm), and (c) 0.5 m DOI (resistivity range 200–500 Ωm) [Colour figure can be viewed at wileyonlinelibrary.com]

The apparent resistivity data obtained from the conductivity data collected using the CMD and GEM-2 instruments, in particular, considering the quadrature component of the field, were separately analysed for recognizing and removing any DC ‘static shifts’, outliers and short-wavelength noises. Then, the datasets are interpolated using SURFER 11 software (Golden Software), and, thanks to the GPS reference, these were overlapped to the satellite view (from Google Earth). In this way, the apparent resistivity maps shown in the images from Figure 12 to Figure 15 were obtained.

It should be noted that only in Figures 12 and 13 for the maps at different frequencies, obtained with the measurements made with the GEM-2 it was possible to use the same range of resistivity, whereas for the images of the apparent resistivity maps, shown in Figures 14 and 15 relating to different DOI, this was not possible because of the different sensitivity of the instrument at different depths. The use of an identical scale of resistivity values, in this case, would have flattened or saturated the signal in some maps compared to others. Therefore, it was decided to keep the resistivity ranges as obtained. It

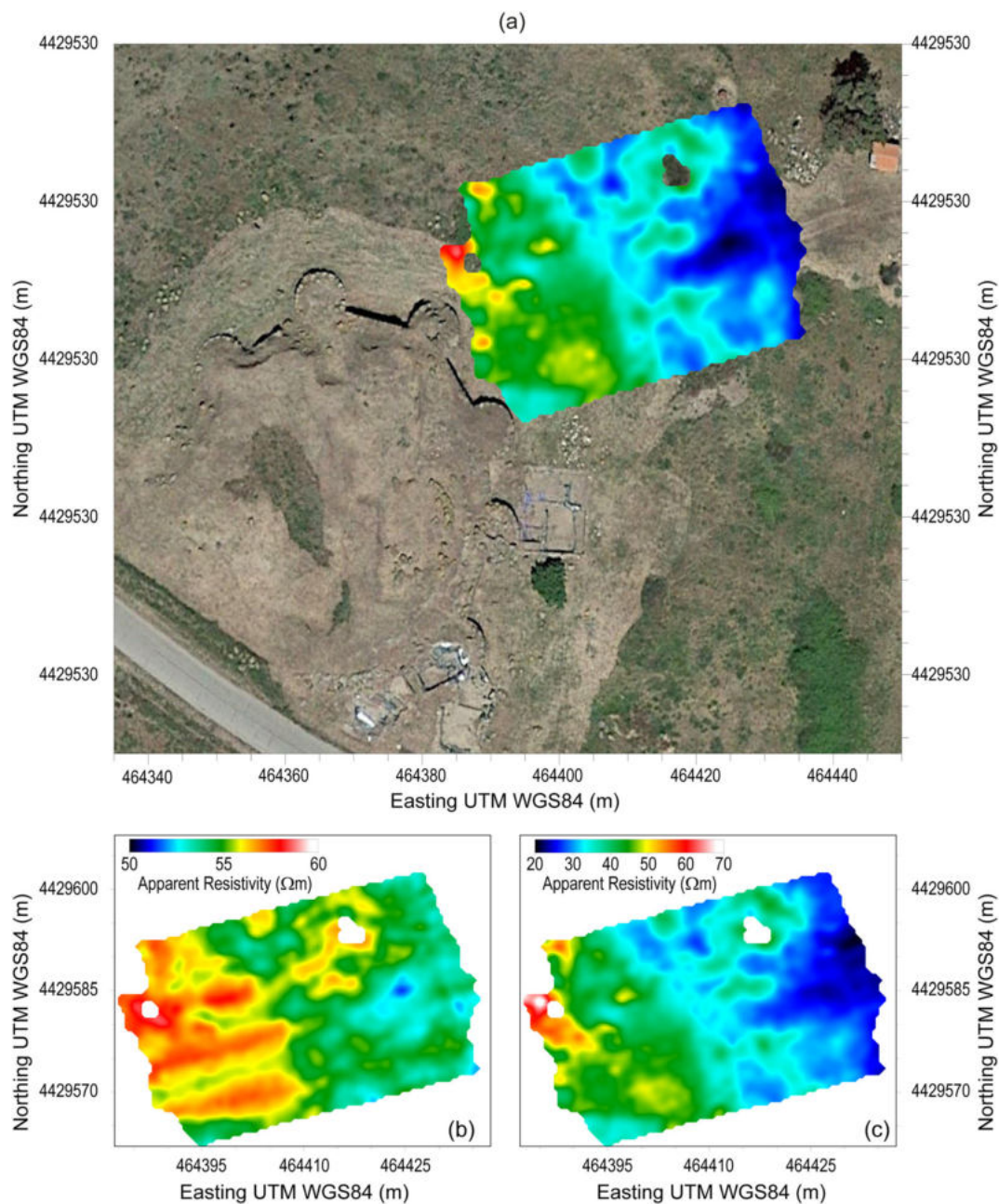


FIGURE 15 Maps of apparent resistivity at the foot of the Nuraghe collected in 2020 using the CMD Mini explorer in HCP configuration over different terrain thicknesses: (a) 1 m DOI (resistivity range 20–60 Ωm), (b) 0.5 m DOI (resistivity range 50–60 Ωm), and (c) 1.8 m DOI (resistivity range 20–70 Ωm) [Colour figure can be viewed at [wileyonlinelibrary.com](https://onlinelibrary.wiley.com)]

should also be noted that due to the different sensitivity of ERT measurements compared to FDEM measurements, to the inversion of the data operated only on ERT measurements, therefore to the different accuracy of the data provided and to the completely different depths of investigation under investigation, the ranges of resistivity values for each method and instrument were chosen identifying the best possible display of anomalies for each dataset. The analysis of the apparent resistivity maps obtained with the two instruments outside the nuraghe makes it clear that the results from the quadrature component made by the CMD Mini explorer (Figure 15) are consistent

with those of the quadrature provided by GEM-2 (Figure 13). It is moreover also evident that the former is more detailed in the definition of anomalies than the latter.

The pattern of alignments identified in this area seems to extend the structures excavated in area F (Figure 6) within the first 1.8 m of depth (Figures 13 and 15). It also matches the anomalies detected by the ERT L4 section in the excavation area (Figure 11).

The measurements carried out with the two EM instruments on top of the nuraghe (Figures 12 and 14) show anomalies not easily comparable with the observations and interpretations discussed using

FIGURE 16 Likely course of the ditch around the Nuraghe as suggested by the ERT anomalies. The ditch probably surrounded the monument entirely but lack of access prevented survey of the southern stretch [Colour figure can be viewed at wileyonlinelibrary.com]



the ERT lines results (Figure 11) because of the different resolution and investigation depth of these different methods. Nevertheless, FDEM measurements on the top of the nuraghe (Figures 12–14) helped in the identification of some shallow circular features in the northern and eastern part of the investigated area, possibly related to the upper part of the internal buried towers, not highlighted by the ERT measurements due to the high electrode spacing here adopted and the consequent low resolution obtained.

4 | CONCLUSIONS

The geophysical measurements conducted at the S'Urachi site between 2018 and 2020 allow us partially to answer the different archaeological questions underlying this study while also highlighting the critical issues related to the application of ERT and FDEM techniques in this context. FDEM measurements were used in 2019 and 2020 for the investigations on the top of the still-buried structure of the nuraghe and in the area adjacent to excavation area F, whereas ERT measurements were conducted over the structure of the nuraghe and around it, thus attempting to provide an answer to the three archaeological questions posed initially. The use of FDEM measurements proved to be ineffective in the analysis of the deeper buried structure of the nuraghe. The probable presence of inhomogeneous material buried in collapse within the structure, the minimal space for the measurements, with numerous surface obstacles (stones and

vegetation) and which prevented acquisition according to a regular geometry, may have contributed to the negative outcome of this application on the top of the nuraghe. More promising and consistent with the evidence of excavation in sector F is instead the application of the FDEM technique to investigate the remains of the habitation area at the base of the nuraghe in the area adjacent to excavation area F. In this context, too, however, a high level of noise in the data is noted, probably related to the presence of landfill materials scattered in the upper part of the subsoil.

Undoubtedly more compelling was the use of the ERT technique. It was possible to investigate both the internal part of the buried structure of the nuraghe and the external parts at the base of the monument. In this way, the sections acquired between 2018 and 2019 made it possible to detect the potential presence of areas of high resistivity inside the unexcavated structure of the nuraghe and areas of very low resistivity. The former might be attributable to the presence of collapse zones with extensive open, that is, air-filled spaces, as opposed to the latter, where water and/or very fine and conductive soils (e.g., clayey soils) could likely have filled in the spaces between the walls of the inner structures. Following this information, one could therefore hypothesize the presence of spaces inside the structure, such as multiple rooms and one or more courtyards, which are common in Nuragic complexes. We may also have picked up an internal wall, as indicated by the low resistivity values in the inner part of the structure. With regard to the external areas and therefore to the questions concerning the presence of a ditch around the nuraghe,

the ERT sections do indeed show the presence of conductive anomalies in areas compatible with the crossing of this hypothetical structure (Figure 16). Finally, although the few sections acquired in correspondence with the excavation area F and nearby positions only allow for highlighting limited anomalies attributable to the presence of structural remains, the data collected seem to corroborate the FDEM measurements.

The ERT and FDEM data acquired at S'Urachi in 2018–2020, therefore, provide indications for both further geophysical investigations and specific test excavations in correspondence with the areas in which the ditch around the nuraghe appears to be present (Figure 16). The interpretation and immediate validation of the data related to the buried structure of the nuraghe are problematic, for which a future 3D ERT survey campaign could be helpful to complete what has already been acquired, whereas the acquisition of seismic refraction data could validate some of the hypotheses about the internal buried structure of the central nuraghe. Even if the FDEM measurements did not yield new data for the buried structure of the nuraghe, they nevertheless demonstrate that the domestic structures under excavation in area F extend further east; they also confirm the electrical tomography suggestion that there are other structures buried below these Punic houses.

ACKNOWLEDGEMENTS

The authors thank Luigi Noli, Mario Sitzia, Nicole Pizzolato and Eugenio Bigo for the support during the geophysical fieldwork. This research was funded by Brown University, Joukowsky Institute for Archaeology and the Ancient World; Loeb Classical Library Foundation (Harvard University) and the Comune and Museo Civico di San Vero Milis.

CONFLICT OF INTEREST

The authors declare no conflict of interest.

AUTHOR CONTRIBUTIONS

Rita Deiana dealt with the conceptualization, data acquisition, data processing, supervision, validation, visualization, and writing—original draft; Gian Piero Deidda dealt with the conceptualization, data acquisition, data processing, validation, visualization, and writing—original draft; Enrique Díes Cusí dealt with the validation, and visualization; Peter van Dommelen dealt with the conceptualization, data acquisition, data processing, funding acquisition, supervision, validation, visualization, and writing—original draft; Alfonso Stiglitz dealt with the conceptualization, funding acquisition, supervision, validation, and writing—original draft.

DATA AVAILABILITY STATEMENT

Data used in this paper will be made accessible on the University of Padova Data Repository (http://bibliotecadigitale.cab.unipd.it/en/publishing_EN/Research%20Data%20Unipd).

ORCID

Rita Deiana  <https://orcid.org/0000-0002-3736-9181>

REFERENCES

- Batayneh, A. (2011). Archaeogeophysics—archaeological prospection—A mini review. *Journal of King Saud University - Science*, 23, 83–89. <https://doi.org/10.1016/j.jksus.2010.06.011>
- Berge, M. A., & Drahor, M. G. (2011a). Electrical resistivity tomography investigations of multi-layered archaeological settlements: Part I—Modelling. *Archaeological Prospection*, 18(3), 159–171.
- Berge, M. A., & Drahor, M. G. (2011b). Electrical resistivity tomography investigations of multilayered archaeological settlements: Part II—A case from old Smyrna Hoyuk Turkey. *Archaeological Prospection*, 18(4), 291–302. <https://doi.org/10.1002/arp.423>
- Bernardes, P., Alves, M., Pereira, B., Madeira, J., Martins, M., & Fontes, L. (2017). Visualization of ERT data for archaeological purposes. doi: 10.2312/gch.20171294 *Conference: Eurographics workshop on graphics and cultural heritage*, at Graz, Austria.
- Binley, A. 2008: ProfileR version 2.5, <http://www.es.lanccs.ac.uk/people/amb/Freeware/ProfileR/profiler.zip>, accessed 20 July 2019.
- Bonsall, J., Fry, R., Gaffney, C., Armit, I., Beck, A., & Gaffney, V. (2013). Assessment of the CMD mini-explorer, a new low-frequency multi-coil electromagnetic device, for archaeological investigations. *Archaeological Prospection*, 20, 219–231. <https://doi.org/10.1002/arp.1458>
- Clark, A. (2000). *Seeing beneath the soil: Prospection methods in archaeology*. London: Routledge. Reprinted. Originally published 1990, B.T. Batsford Ltd., London
- Dabas, M., & Tabbagh, A. (2003). *A comparison of EMI and DC methods used in soil mapping - theoretical considerations for precision agriculture*. Wageningen Academic Publishers.
- Daily, W. A., Ramirez, A., Binley, A., & LaBrecque, D. (2004). Electrical resistivity tomography. *Leading Edge*, 23(5), 438–442. <https://doi.org/10.1190/1.1729225>
- De Smedt, P., Meirvenne, M., Saey, T., Baldwin, E., Gaffney, C., & Gaffney, V. (2014). Unveiling the prehistoric landscape at Stonehenge through multi-receiver EMI. *Journal of Archaeological Science*, 50, 16–23. <https://doi.org/10.1016/j.jas.2014.06.020>
- De Smedt, P., Saey, T., Lehouck, A., Stichelbaut, B., Meerschman, E., Islam, M. M., Van De Vijver, E., & Meirvenne, M. (2013). Exploring the potential of multi-receiver EMI survey for geoarchaeological prospection: A 90 ha dataset. *Geoderma*, 40, 1260–1267.
- Deiana, R. (2019). The contribution of geophysical prospecting to the multidisciplinary study of the sarno baths, Pompeii. *Journal of Cultural Heritage*, 40, 274–279. <https://doi.org/10.1016/j.culher.2019.04.018>
- Deiana, R., Bonetto, J., & Mazzariol, A. (2018). Integrated electrical resistivity tomography and ground penetrating radar measurements applied to tomb detection. *Surveys in Geophysics*, 39(6), 1081–1105. <https://doi.org/10.1007/s10712-018-9495-x>
- Deiana, R., Leucci, G., & Martorana, R. (2018). New perspectives on geophysics for archaeology: A special issue. *Surveys in Geophysics*, 39(6), 1035–1038. <https://doi.org/10.1007/s10712-018-9500-4>
- Deiana, R., Vicenzutto, D., Deidda, G. P., Boaga, J., & Cupitò, M. (2020). Remote sensing, archaeological, and geophysical data to study the Terramare settlements: The case study of Fondo Paviani (northern Italy). *Remote Sensing*, 12, 2617. <https://doi.org/10.3390/rs12162617>
- Depalmas, A. (2015). I nuraghi. Le torri dell'isola. In M. Minoja, G. F. Salis, & L. Usai (Eds.), *L'isola delle torri. Giovanni Lilliu e la Sardegna nuragica* (pp. 76–83). Sassari: Carlo Delfino.
- Depalmas, A., & Melis, R. T. (2010). The Nuragic people: Their settlements, economic activities and use of the land, Sardinia, Italy. In P. Martini & W. Chesworth (Eds.), *Landscapes and societies* (pp. 167–186). Dordrecht and New York: Springer. <https://doi.org/10.1007/978-90-481-9413-1>
- El-Qady, G., Metwaly, M., & Drahor, M. (2019). Geophysical techniques applied in archaeology. In G. El-Qady & M. Metwaly (Eds.), *Archaeogeophysics: State of the art and case studies* (pp. 1–25). Springer Nature. https://doi.org/10.1007/978-3-319-78861-6_1

- Gosner, L., & Smith A. (2018). Landscape use and local settlement at the nuraghe S'Urachi (West Central Sardinia): Results from the first two seasons of site survey (2014-2015). FOLDER sur-2018.7: www.fastionline.org/docs/FOLDER-sur-2018-7.pdf
- Himi, M., Armendariz, A., Teira, L., González, J., Ibáñez, J. J., Haïdar-Boustani, M., & Casas, A. (2016). Geophysical and archaeological evidences of buried Epipalaeolithic, Neolithic, bronze age and Roman architecture in west-Central Syria. *Archaeological Prospection*, 23, 273–285. <https://doi.org/10.1002/arp.1543>
- James, I. T., Waine, T. W., Bradley, R. I., Taylor, J. C., & Godwin, R. J. (2003). Determination of soil type boundaries using electromagnetic induction scanning techniques. *Biosystems Engineering*, 86(4), 421–430. <https://doi.org/10.1016/j.biosystemseng.2003.09.001>
- Johnson, P. (2012). Sant'Imbenia: geophysical survey in the environs of the Nuragic settlement. In M. B. Cocco, A. Gavini, & A. Ibbà (Eds.), *Trasformazione Dei paesaggi del potere nell'Africa settentrionale fino alla fine del mondo antico. Scontri, integrazioni, transizioni e dinamiche insediative. Nuove prospettive dalla ricerca (Atti del XIX Convegno di studio, Sassari-Alghero, 16-19 dicembre 2010)* L'Africa Romana 19: 1753–70. Rome: Carocci.
- Kvamme, K. L. (2003). Geophysical surveys as landscape archaeology. *American Antiquity*, 68(3), 435e457.
- LaBrecque, D. J., Miletto, M., Daily, W., Ramirez, A., & Owen, E. (1996). The effects of noise on Occam's inversion of resistivity tomography data. *Geophysics*, 61, 538–548. <https://doi.org/10.1190/1.1443980>
- Lilliu, G. (1988). *La civiltà Dei Sardi dal Paleolitico all'età Dei nuraghi* (3rd ed.). Turin: Nuova ERI.
- Lorrio, A. (2012). Fosos en los sistemas defensivos del Levante ibérico (siglos VIII-II a.C.). *Revista d'Arqueologia de Ponent*, 22, 59–86.
- Madrigali, E., Gosner, L., Hayne, J., Nowlin, J., & Ramis, D. (2019). Tradizioni e interazioni nella quotidianità dell'età del ferro. Nuove evidenze da Su Padriheddu (san Vero Milis, OR). *Quaderni Della Soprintendenza Archeologia, Belle Arti e Paesaggio per la città Metropolitana di Cagliari e le Province di Oristano e Sud Sardegna*, 30, 107–126.
- Minoja, M., Salis, G. F., & Usai, L. (2015). *L'isola delle torri. Giovanni Lilliu e la Sardegna nuragica*. Sassari: Carlo Delfino.
- Mol, L., & Preston, P. (2010). The writing's in the wall: A review of new preliminary applications of electrical resistivity tomography within archaeology. *Archaeometry*, 52(6), 1079–1095.
- Papadopoulos, N. G., Tsourlos, P., Tsokas, G. N., & Sarris, A. (2006). Two-dimensional and three-dimensional resistivity imaging in archaeological site investigation. *Archaeological Prospection*, 13, 163–181. <https://doi.org/10.1002/arp.276>
- Parasnis, D. S. (1988). Reciprocity theorems in geoelectric and geoelectromagnetic work. *Geoexploration*, 25, 177–198. [https://doi.org/10.1016/0016-7142\(88\)90014-2](https://doi.org/10.1016/0016-7142(88)90014-2)
- Rhoades, J. D., Lesch, S. M., Shouse, P. J., & Alves, W. J. (1989). New calibrations for determining soil electrical conductivity depth relations from electromagnetic measurements. *Soil Science Society of America Journal*, 53, 74–79. <https://doi.org/10.2136/sssaj1989.03615995005300010014x>
- Saey, T., De Smedt, P., Meerschman, E., Islam, M. M., Meeuws, F., Van De Vijver, E., Lehouck, A., & Van Meirvenne, M. (2012). Electrical conductivity depth modeling with a multireceiver EMI sensor for prospecting archaeological features. *Archaeological Prospection*, 19, 21–30. <https://doi.org/10.1002/arp.425>
- Saey, T., Van Meirvenne, M., De Smedt, P., Neubauer, W., Trinks, I., Verhoeven, G., & Seren, S. (2013). Integrating multi-receiver electromagnetic induction measurements into the interpretation of the soil landscape around the school of gladiators at Carnuntum. *European Journal of Soil Science*, 64, 716–727. <https://doi.org/10.1111/ejss.12067>
- Schmidt, A. (2001). *Geophysical data in archaeology: A guide to good practice*. Oxford: Oxbow Books.
- Simon, F.-X., Tabbagh, A., Donati, J., & Sarris, A. (2018). Permittivity mapping in the VLF-LF range using a multi-frequency EMI device: First tests in archaeological prospection. *Near Surface Geophysics*, 17, 27–41.
- Simon F.-X., Tabbagh A., Sarris A., Thiesson J., 2014. Practical assessment of a multifrequency Slingram EMI for archaeological prospection. Proceedings of the 42nd annual conference on computer applications and quantitative methods in Archaeology, CAA 2014, Archaeopress, Oxford, 43–52.
- Simon, F.-X., Tabbagh, A., Thiesson, J., & Sarris, A. (2015). Mapping of quadrature magnetic susceptibility/magnetic viscosity of soils by using multi-frequency EMI. *Journal of Applied Geophysics*, 120, 36–47. <https://doi.org/10.1016/j.jappgeo.2015.06.007>
- Stiglitz, A. (2019). L'isola più grande del mondo. Incontri mediterranei e oltre. In C. del Vais, M. Guirguis, & A. Stiglitz (Eds.), *Il tempo Dei Fenici. Incontri in Sardegna dall'VIII al III secolo a.C* (pp. 18–25). Nuoro: Ilisso.
- Stiglitz, A., Dies Cusi, E., Ramis, D., Roppa, A., & van Dommelen, P. (2015). Intorno al nuraghe: Notizie preliminari sul Progetto S'Urachi (san Vero Milis, OR). *Quaderni Della Soprintendenza Archeologica per le Province di Cagliari e Oristano*, 26, 191–218.
- Stiglitz, A., Puliga, B., Usai, A., Carboni, S., & Lecca, L. (2012). Il complesso di S'Urachi e l'insediamento di Su Padriheddu (San Vero Milis - OR). Indagini interdisciplinari per un approccio al tema delle relazioni tra gli ultimi nuragici e i primi fenici. In C. Lugliè (Ed.), *Preistoria e Protostoria della Sardegna (Atti della XLIV Riunione, novembre 2009)* III: Comunicazioni. Atti delle Riunioni Scientifiche 44: 921–6. Rome: L'Erma di Bretschneider.
- Tabbagh, A. (1986). Applications and advantages of the Slingram electromagnetic method for archaeological prospecting. *Geophysics*, 51, 576–584. <https://doi.org/10.1190/1.1442112>
- Tabbagh, A. (1990). *Electromagnetic prospecting*. In I. Scollar (Ed.), *Archaeological prospecting and remote sensing*. Cambridge: Cambridge University Press.
- Thiesson, J., Dabas, M., & Flageul, S. (2009). Detection of resistive features using towed slingram electromagnetic induction instruments. *Archaeological Prospection*, 16, 103–109. <https://doi.org/10.1002/arp.350>
- Tsourlos, P. I., Szymanski, J., & Tsokas, G. N. (1999). The effect of terrain topography on commonly used resistivity arrays. *Geophysics*, 64, 64–1363. <https://doi.org/10.1190/1.1444640>
- Tsourlos, P. I., & Tsokas, G. N. (2011). Non-destructive electrical resistivity tomography survey at the south walls of the acropolis of Athens. *Archaeological Prospection*, 18, 173–186.
- Ullrich, B., Günther, T., & Rücker, C. (2007). Electrical resistivity tomography methods for archaeological prospection. Conference: Layers of perception. Proceedings of the 35th international conference on computer applications and quantitative methods in archaeology (CAA), Berlin, April 2–6, 2007.
- Vacilotto, A., Deiana, R., & Mozzi, P. (2020). Understanding ancient landscapes in the venetian plain through an integrated Geoarchaeological and geophysical approach. *Remote Sensing*, 12, 2973. <https://doi.org/10.3390/rs12182973>
- van Dommelen, P., Dies Cusi, E., Gosner, L., Hayne, J., Pérez Jordà, G., Ramis, D., Roppa, A., & Stiglitz, A. (2018). Un millennio di storie: Nuove notizie preliminari sul progetto S'Urachi (san Vero Milis, OR), 2016-2018. *Quaderni Della Soprintendenza Archeologia, Belle Arti e Paesaggio per la città Metropolitana di Cagliari e le Province di Oristano e Sud Sardegna*, 29, 141–166.
- van Dommelen, P., Ramis, D., Roppa, A., & Stiglitz, A. (2020). Progetto S'Urachi: incontri culturali intorno a un nuraghe di età fenicio-punica. In S. Celestino Pérez & E. Rodríguez González (Eds.), *Un viaje entre el Oriente y el Occidente del Mediterráneo. Actas del IX Congreso Internacional de Estudios Fenicios y Púnicos. (MYTRA 5)* (pp. 1627–1636). Mérida: CSIC.

- Vanzetti, A., Castangia, G., Depalmas, A., Ialongo, N., Leonelli, V., Perra, M., & Usai, A. (2013). Complessi fortificati della Sardegna e delle isole del mediterraneo occidentale nella protostoria. In G. Bartoloni & L. M. Michetti (Eds.), *Scienze dell'Antichità 19.2-3 (Atti del Convegno Mura di legno, mura di terra, mura di pietra: Fortificazioni nel Mediterraneo antico)* (pp. 83–123). Roma: Ed. QUASAR.
- Walker, A. R. (2000). Multiplexed resistivity survey at the Roman town of Wroxeter. *Archaeological Prospection*, 7, 119–132. [https://doi.org/10.1002/1099-0763\(200006\)7:2%3C119::AID-ARP147%3E3.0.CO;2-W](https://doi.org/10.1002/1099-0763(200006)7:2%3C119::AID-ARP147%3E3.0.CO;2-W)
- Webster, G. (2015). *The archaeology of Nuragic Sardinia* Monographs in Mediterranean Archaeology 14. Sheffield: Equinox.
- Wynn, J. (1986). A review of geophysical methods in archaeology. *Geoarchaeology*, 1, 245–257. <https://doi.org/10.1002/gea.3340010302>

How to cite this article: Deiana, R., Deidda, G. P., Cusí, E. D., van Dommelen, P., & Stiglitz, A. (2021). FDEM and ERT measurements for archaeological prospections at Nuraghe S'Urachi (West-Central Sardinia). *Archaeological Prospection*, 1–18. <https://doi.org/10.1002/arp.1838>